PERFORMANCE PREDICTION OF ENERGY EFFICIENT PERMANENT SPLIT CAPACITOR RUN SINGLE PHASE INDUCTION MOTOR

Vijay Kumar GHIAL[1] Lalit Mohan SAINI[2] Jasbir Singh SAINI[3]
[1] Electrical Engineering Department, National Institute of Technology, Kurukshetra, India.
Email: vijayghial@yahoo.co.in
[2] Electrical Engineering Department, National Institute of Technology, Kurukshetra, India.
Email: lmsaini@gmail.com
[3]Electrical Engineering Department, Deenbandhu Chhotu Ram University of Science & Technology, Murthal, Sonepat, India.
Email: jssain@rediffmail.com

Abstract: *The performance of permanent-split capacitor-run single-phase induction motor can be evaluated from the equivalent circuit parameters, which are derived from dc test, no-load test, locked-rotor test and the winding ratio test. In the present work, the conventional turns ratio has been replaced with computed complex voltage ratio for performance prediction of the ac voltage controller fed capacitor-run motor, at different firing angles of triac. Two different energy efficient experimental schemes, namely traditional phase angle control scheme (with ac voltage controller in series with both main and auxiliary windings) and advanced phase angle control scheme (with ac voltage controller in series with main winding alone), are used for performance observation of the motor. It is observed that for both the schemes, the proposed performance prediction method gives performance variables values closer to the experimental observations in comparison to those obtained using the conventional performance prediction methods. Further, it is also demonstrated that although the conventional parameter estimation and performance prediction methods did not show superiority of the advanced ac voltage control scheme over the traditional one, yet the proposed method does so.*

Keywords: *AC Motors, Capacitor motors, Equivalent circuits, Induction motors, Parameter estimation, Power semiconductor switches.*

1. INTRODUCTION

Single phase motors are small motors, mostly built in the fractional horse power range. These types of motors are used for many types of equipment in homes, offices, shops and factories. In fact, the number of single-phase (fractional horsepower) motors in use today far exceeds the number of integral horsepower motors of all types.

The IEEE Standard 114-1982 [1] and 114-2001 [2] provide the testing methods for Single Phase Induction Motor (SPIM), but these do not provide a method of extracting the parameters of Permanent-Split Capacitor-Run Single-Phase Induction Motor (PSCRSPIM). For parameter extraction of SPIM, except for capacitor run motor, the no-load and locked-rotor tests are made with the auxiliary winding kept open. In capacitor-run motor, however, auxiliary winding parameters also contribute in these test results even though rest of the procedure, to find the main and auxiliary winding parameters, remains the same as that of plain SPIM [3]. The conventional methods [4-6] calculate the performance variables by taking turns ratio of SPIM as a scalar quantity, which is measured using the winding ratio test. However, the resulting performance variables (line current, power factor and power) give error vis-a-vis experimental values, which in turn, fallaciously compute the efficiency of the PSCRSPIM.

Different schemes have been proposed to find out the equivalent circuit parameters and performance variables for performance prediction of SPIM [4-30]. A detailed review of induction motor parameter estimation techniques with experimental and simulation illustrations, related to online and offline parameter estimation techniques has been reported in [7]. Some researchers have proposed online parameter estimation techniques such as least mean square technique, particle swam optimization technique, averaging analysis technique, elementary layer method, direct-on-line starting and natural slowdown tests etc.[8-13], while others have proposed offline parameter extraction methods such as vector constructing method, vector control scheme using offline genetic-algorithm routine, Lyapunov function based state observer, direct torque-controlled space-vector-modulated method, extrapolative, equation error and generalized identification method etc.[14-27]. Although various offline parameter-estimation techniques have been proposed for single- and three-phase IMs as because the offline identification is typically easier and more reliable than online methods, yet a little work has been reported for the performance prediction of PSCRSPIM [28-30]. This paper is an advancement of the previous work [3] in which the major thrust was on proposing a new complex turn ratio (named as CCVR) which was used to estimate the parameter and hence the performance variables. However, the present paper lays emphasis on evaluation of efficiency of PSCRSPIM by adopting two different energy efficient experimental schemes and using the proposed methodology. The application of the proposed theory is based on the assumption that SPIM can be represented as an ideal transformer, with such a transformation ratio that for which voltages are transformed in the direct ratio of turns, currents in the inverse ratio and impedances in direct ratio squared; power and volt amperes are unchanged.

In this paper, in contrast to the conventional approach, the parameters of main and auxiliary windings are extracted individually and then using the Computed Complex Voltage Ratio (CCVR), the equivalent circuit of PSCRSPIM is developed. The performance variables of the motor are then computed at different firing angles of triac. For comparative study, two energy efficient experimental schemes are applied on PSCRSPIM, one of which is conventional phase angle control scheme and the other one is an advanced phase angle control scheme. The computed efficiency of the motor for the advanced scheme is shown to be better only using the proposed performance prediction method.

2. PERMANENT-SPLIT CAPACITOR-RUN SINGLE-PHASE INDUCTION MOTOR

The PSCRSPIM has two windings, one is known as main winding and the other is called auxiliary winding, as shown in Fig. 1. A capacitor is connected in series with the auxiliary winding and both the windings are connected in parallel with an AC supply source.

These windings are geometrically displaced in such a way that the magnetic fields produced in space are 90^0 apart. The magnetic field produced by the motor, that pulsates in time, but, is stationary in space, can be resolved into two revolving magnetic fields that are equal in magnitude, but, revolve synchronously in opposite directions. The induced e.m.f.s in the rotor due to the two revolving fields are in opposition to each other.

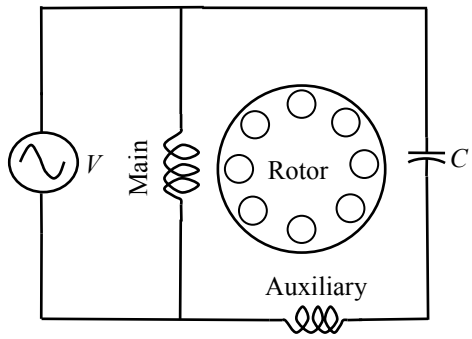

Fig. 1. Schematic representation of PSCRSPIM.

The slip in either forward or backward branches of the rotor is same at standstill. Therefore, the starting torque developed by each revolving field is the same and the net torque developed by the motor is zero and hence SPIM is not self-starting. An induction motor can be made self starting, if the two windings are placed in space quadrature and are connected in parallel to a single phase source, but, impedances of two windings are made unequal to produce out-of-phase currents which, in turn, set up a net unbalanced revolving field.

3. Proposed Performance Estimation of PSCRSPIM

In the formal practice, for performance prediction of the PSCRSPIM, the parameters of the main winding are first computed and then main winding referred auxiliary winding parameters are computed using the turns ratio. However, in the present work, for computation of efficiency of the motor, the total input impedances of both the windings are computed separately using the no-load and locked rotor tests and using the computed complex voltage ratio (CCVR) instead of the conventional turns ratio.

The conventional scalar turns ratio, a, in terms of constant voltage transformation ratio is given by:

$$\frac{N_2}{N_1} = \frac{I_{primary}}{I_{\sec ondary}} = \frac{V_{\sec ondary}}{V_{primary}} = a \tag{1}$$

where, N_1 and N_2 are the no. of turns of main and auxiliary windings, respectively.

For the complex transformation ratio, the main and auxiliary windings self induced e.m.f.s, ($\overline{E}_{mc}$ and $\overline{E}_{ac}$) at rated voltage, can be computed as [3]:

$$\overline{E}_{mc} = \bar{I}_1\left(\overline{Z}_{insm}\right) \tag{2}$$

$$\overline{E}_{ac} = \bar{I}_2\left(\overline{Z}_{insa}\right) \tag{3}$$

where, $\overline{Z}_{insm}$, $\overline{Z}_{insa}$ are the total input impedances and $\bar{I}_1$, $\bar{I}_2$ are the phasor currents of the main and auxiliary winding equivalent circuits, respectively.

As on application of rated voltage on the one winding, such e.m.f. is supposed to be induced across the other winding, which makes the currents of two windings in inverse ratio of turns, therefore, equations (2) and (3) can be rewritten as [3]:

$$\overline{E}_{mc} = \frac{\bar{I}_2}{\bar{a}_2}\left(\overline{Z}_{insm}\right) \tag{4}$$

$$\overline{E}_{ac} = \frac{\bar{I}_1}{\bar{a}_1}\left(\overline{Z}_{insa}\right) \tag{5}$$

The computed voltage induced across the one winding would then be in the direct ratio of rated voltage applied across the other winding. The turns ratio in terms of complex voltage transformation ratio thus can be obtained as:

$$\frac{N_2}{N_1} = \frac{\overline{E}_{ac}}{V_m} = \bar{a}_1 \tag{6}$$

$$\frac{N_2}{N_1} = \frac{V_a}{\overline{E}_{mc}} = \bar{a}_2 \tag{7}$$

where, V_m and V_a are line voltages applied to main and auxiliary winding, respectively.

Multiplying equations (6) and (7), the computed complex voltage ratio CCVR, $\bar{a}$, is thus given by [3]:

$$\bar{a} = \sqrt{\frac{\overline{E}_{ac}}{V_m}\frac{V_a}{\overline{E}_{mc}}} \tag{8}$$

The scalar turns ratio, a, will now be replaced with this observed complex voltage ratio, $\bar{a}$, termed as CCVR.

This transformation ratio is then used for developing the complete equivalent circuit as shown in Fig. 2 and for evaluating the performance variables and hence the efficiency of PSCRSPIM.

The steady state mathematical model of the motor consists of the system of equations which govern its steady state operation under all operating conditions. As shown in Fig. 2, the following equations can be written [3]:

$$V_m = \bar{I}_m\overline{Z}_{sm} + \overline{E}_{fm} + \overline{E}_{bm} - j\frac{\overline{E}_{fa}}{\bar{a}} + j\frac{\overline{E}_{ba}}{\bar{a}} \tag{9}$$

$$V_a = \bar{I}_a\left(\overline{Z}^*_{sa} + \overline{Z}_c\right) + \overline{E}_{fa} + \overline{E}_{ba} + j\bar{a}\overline{E}_{fm} - j\bar{a}\overline{E}_{bm} \tag{10}$$

where:

$$\overline{E}_{fm} = \overline{Z}_{fm}\bar{I}_m \tag{11}$$

$$\overline{E}_{bm} = \overline{Z}_{bm}\bar{I}_m \tag{12}$$

$$\overline{E}_{fa} = \bar{a}^2\overline{Z}_{fa}\bar{I}_a \tag{13}$$

$$\bar{E}_{ba} = \bar{a}^2 \bar{Z}_{ba} \bar{I}_a \quad (14)$$

The main and auxiliary winding voltages are calculated by the application of Kirchhoff's voltage law to the equivalent circuit. Substituting from equations (11)-(14) into equations (9) and (10) yields:

$$V_m = \left(\bar{Z}_{sm} + \bar{Z}_{fm} + \bar{Z}_{bm}\right)\bar{I}_m - j\bar{a}\left(\bar{Z}_{fm} - \bar{Z}_{bm}\right)\bar{I}_a \quad (15)$$

$$V_a = j\bar{a}\left(\bar{Z}_{fm} + \bar{Z}_{bm}\right)\bar{I}_m + \left(\bar{Z}^*_{sa} + \bar{Z}_c + \bar{a}^2\left(\bar{Z}_{fm} + \bar{Z}_{bm}\right)\right)\bar{I}_a \quad (16)$$

Main and auxiliary winding currents ($\bar{I}_m$ and $\bar{I}_a$) can be obtained by solving (15), (16) as follows:

$$\bar{I}_m = \frac{V_m\left(\bar{Z}_{22} - \bar{Z}_{12}\right)}{\bar{Z}_{11}\bar{Z}_{22} - \bar{Z}_{12}\bar{Z}_{21}} \quad (17)$$

$$\bar{I}_a = \frac{V_a\left(\bar{Z}_{11} - \bar{Z}_{21}\right)}{\bar{Z}_{11}\bar{Z}_{22} - \bar{Z}_{12}\bar{Z}_{21}} \quad (18)$$

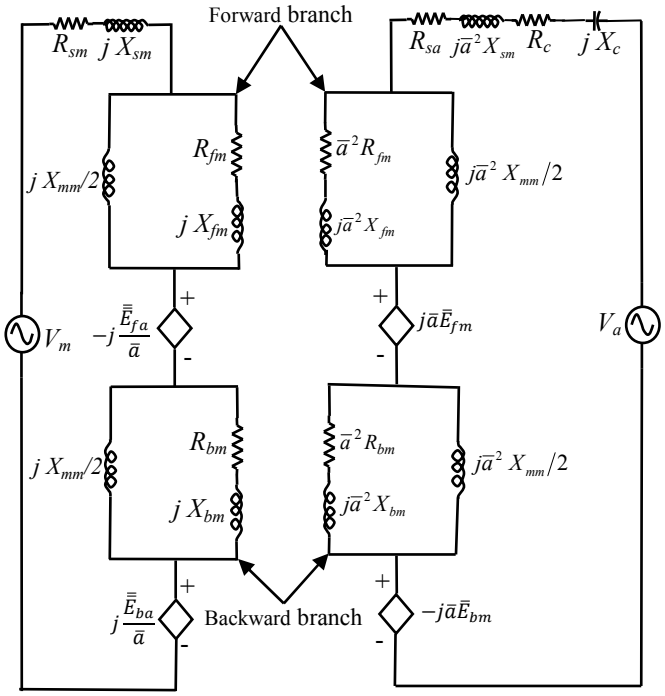

Fig. 2. Proposed equivalent circuit of PSCRSPIM

where, $\bar{Z}_{11}, \bar{Z}_{12}, \bar{Z}_{21}$ and $\bar{Z}_{22}$ are computed as:

$$\bar{Z}_{11} = \bar{Z}_{sm} + \bar{Z}_{fm} + \bar{Z}_{bm} \quad (19)$$

$$\bar{Z}_{12} = -j\bar{a}\left[\bar{Z}_{fm} - \bar{Z}_{bm}\right] \quad (20)$$

$$\bar{Z}_{21} = j\bar{a}\left[\bar{Z}_{fm} - \bar{Z}_{bm}\right] \quad (21)$$

$$\bar{Z}_{22} = \bar{Z}^*_{sa} + \bar{Z}_c + \bar{a}^2\left[\bar{Z}_{fm} + \bar{Z}_{bm}\right] \quad (22)$$

The line current is computed as:

$$I_L = \mathrm{Re}\left[\bar{I}_m + \bar{I}_a\right] \quad (23)$$

On applying input voltage, V, to PSCRSPIM, the power consumed by the motor is given by:

$$P_{in} = VI_L \cos\theta \quad (24)$$

The power factor can be computed as:

$$pf = \cos\theta \quad (25)$$

where, 'θ', is the power factor angle between the applied voltage and the line current.

For PSCRSPIM the total air gap power is defined as:

$$P = P_{gf} - P_{gb} \quad (26)$$

where, P_{gf} and P_{gb} are forward and backward gap powers and are expressed as:

$$P_{gf} = \mathrm{Re}(E_{fm} I_m + j\bar{a} E_{fa} I_a) \quad (27)$$

$$P_{gb} = \mathrm{Re}(E_{bm} I_m + j\bar{a} E_{ba} I_a) \quad (28)$$

By inserting (27) and (28) in to (26), the total air gap power can be obtained as:

$$P_g = P_{gf} - P_{gb} = \left(|I_m|^2 + |\bar{a} I_a|^2\right)\left(R_f - R_b\right) + 2\bar{a}|I_a||I_m|\left(R_f + R_b\right)\sin(\theta_a - \theta_m) \quad (29)$$

The developed power is given by:

$$P_d = \left(1 - S_f\right)P_g \quad (30)$$

The output power is then calculated by subtracting the rotational losses, P_{rot}, from the developed power as follows:

$$P_{out} = P_d - P_{rot} \quad (31)$$

Therefore, the efficiency can be calculated as:

$$\eta = \frac{P_{out}}{P_{in}} \quad (32)$$

In this section, complete equivalent circuit, performance variables including the efficiency of the motor have been calculated using the CCVR.

4. EXPERIMENTAL VALIDATION, RESULTS AND DISCUSSION

In order to verify the theoretical findings, two PSCRSPIMs, as given in table 1, have been taken for study. The performance variables of motors are computed using dc, no-load and locked rotor test results.

Table 1: Specification of fan motors

Motor	Voltage (V)	Power (W)	Frequency (Hz)	Rated speed (rpm)	C (μF)
1	230	65	50	1400	1.57
2	230	160	50	1400	5.0

Two different energy efficient experimental schemes are shown in Fig. 3(a) and 3(b). Fig. 3(a) is the traditional way of phase angle control by using the triac based ac voltage controller between the supply voltage and the motor. An advanced scheme for phase angle control is depicted in Fig. 3(b), in which the triac based ac voltage controller is inserted in series with main winding and the motor auxiliary winding is directly connected to the supply voltage. By varying the firing angle of the triac, different voltages are achieved for both the schemes. The performance variables (such as current, power and power factor) of PSCRSPIMs have been measured with YOKOGAWA WT 3000 Precision power

analyzer and further the efficiency has been deduced theoretically.

The results for current, power and power factor are obtained at different firing angles, using two different energy efficient experimental schemes. The experimental results obtained are then compared with conventional parameter estimation techniques [4-6] and the proposed performance prediction method as shown in Figs. 4-15. In these Figs., the curves corresponding to the bracketed references in the legend are obtained by using the methods given therein. Also, "-1" and "-2" in legend refer to phase angle control scheme-1 and phase angle control scheme-2, respectively.

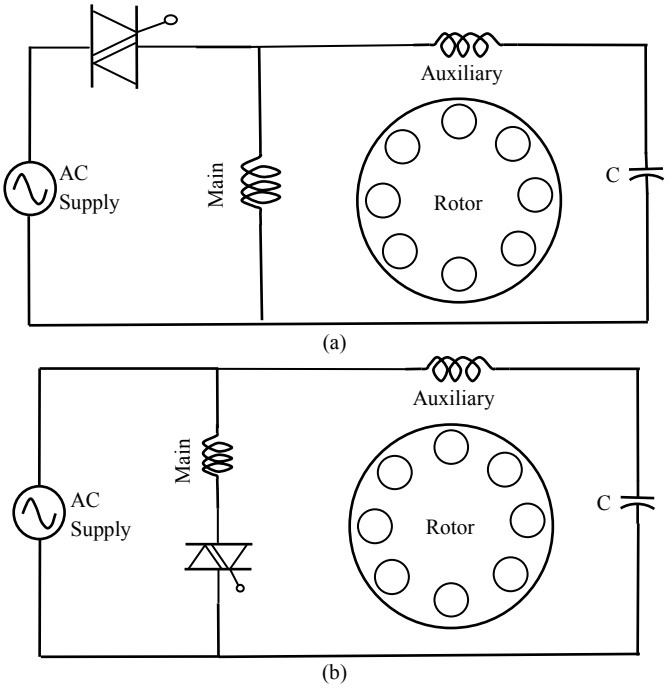

Fig. 3. (a) Traditional phase angle control: Scheme-1.
(b) Advanced phase angle control: Scheme-2.

The inferences that can be drawn from these results are itemized along with the results as below:

- For both the experimental energy efficient schemes, at different firing angles, the performance curves due to the proposed performance prediction method are closer to the experimental ones in comparison to the conventional theoretical parameter estimation methods [4-6], as shown in Figs 4-15.

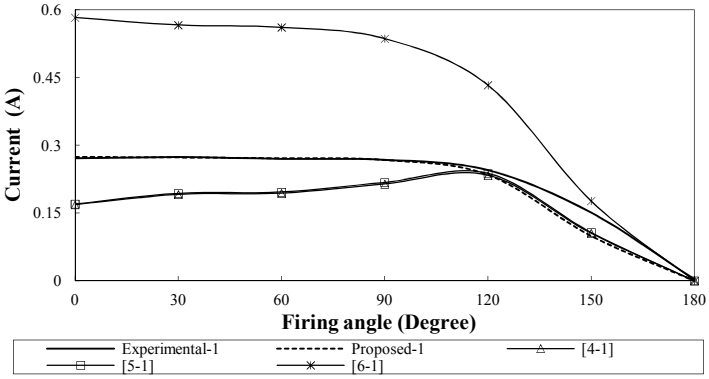

Fig. 4. Current of motor-1 using scheme-1 with proposed and conventional methods, at different firing angles.

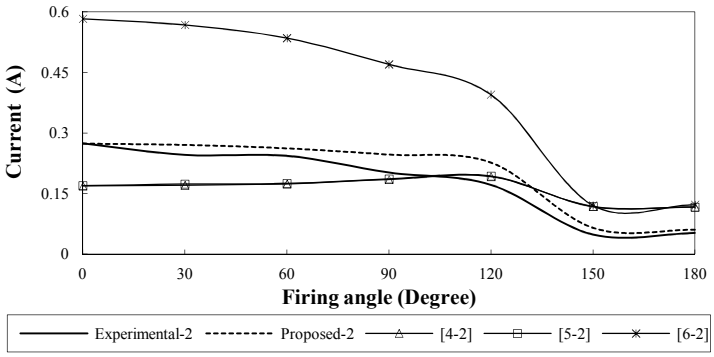

Fig. 5. Current of motor-1 using scheme-2 with proposed and conventional methods, at different firing angles.

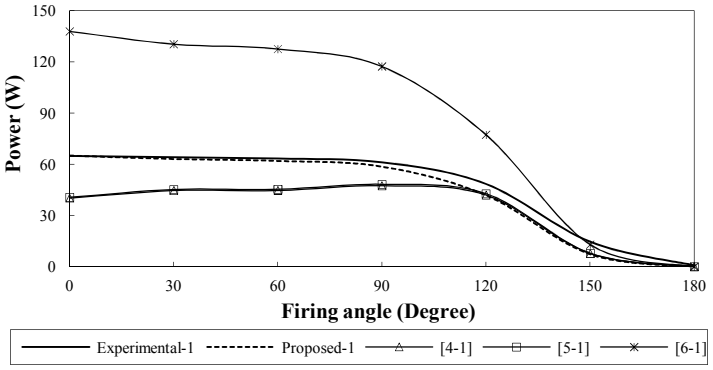

Fig. 6. Power of motor-1 using scheme-1 with proposed and conventional methods, at different firing angles.

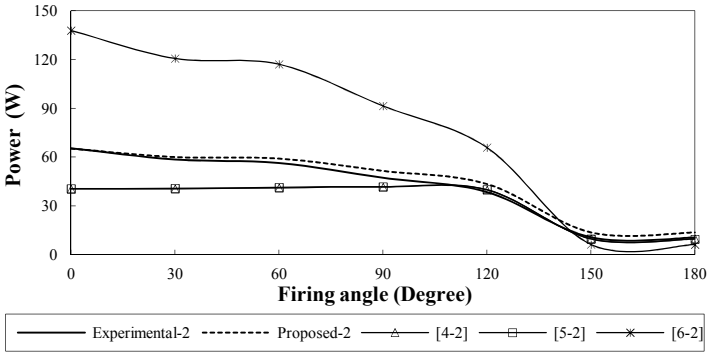

Fig. 7. Power of motor-1 using scheme-2 with proposed and conventional methods, at different firing angles.

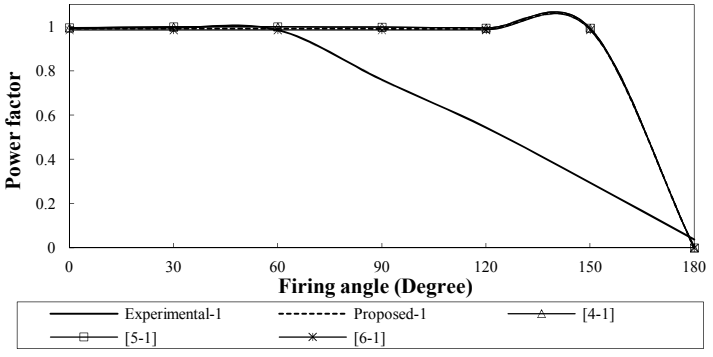

Fig. 8. Power factor of motor-1 using scheme-1 with proposed and conventional methods, at different firing angles.

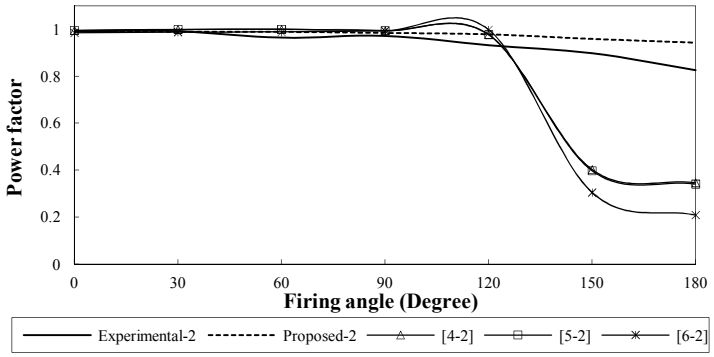

Fig. 9. Power factor of motor-1 using scheme-2 with proposed and conventional methods, at different firing angles.

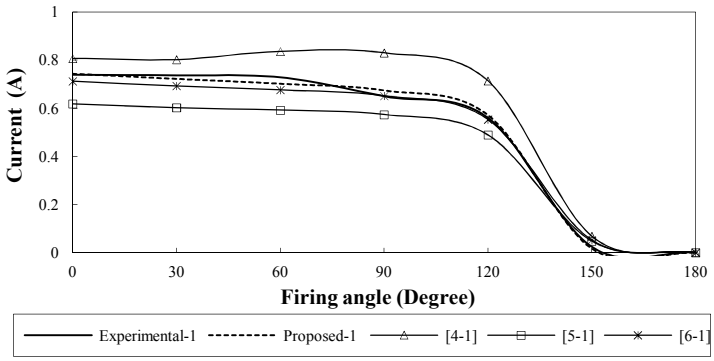

Fig. 10. Current of motor-2 using scheme-1 with proposed and conventional methods, at different firing angles.

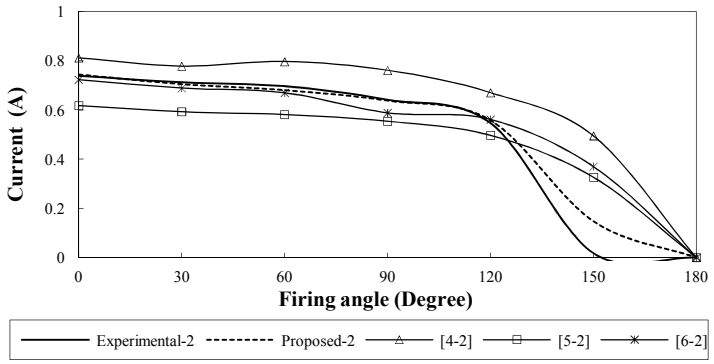

Fig. 11. Current of motor-2 using scheme-2 with proposed and conventional methods, at different firing angles.

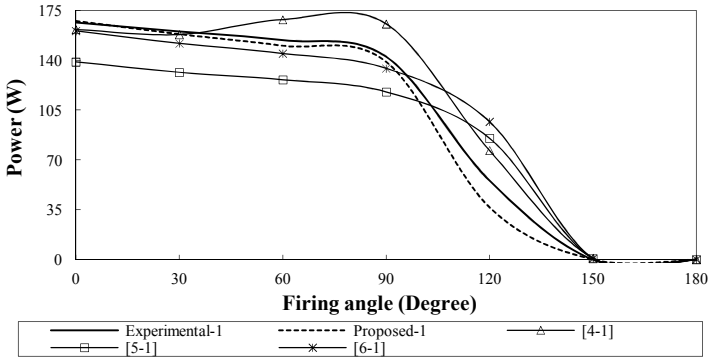

Fig. 12. Power of motor-2 using scheme-1 with proposed and conventional methods, at different firing angles.

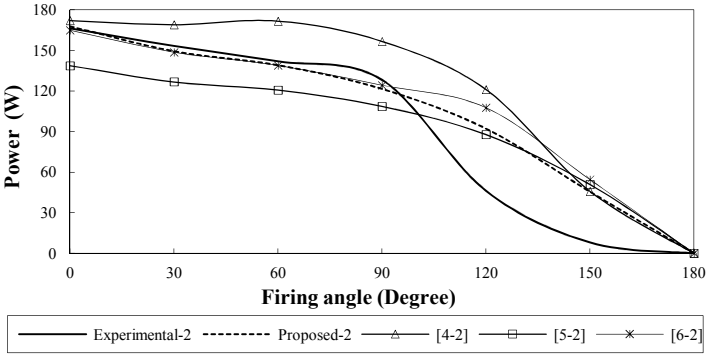

Fig. 13. Power of motor-2 using scheme-2 with proposed and conventional methods, at different firing angles.

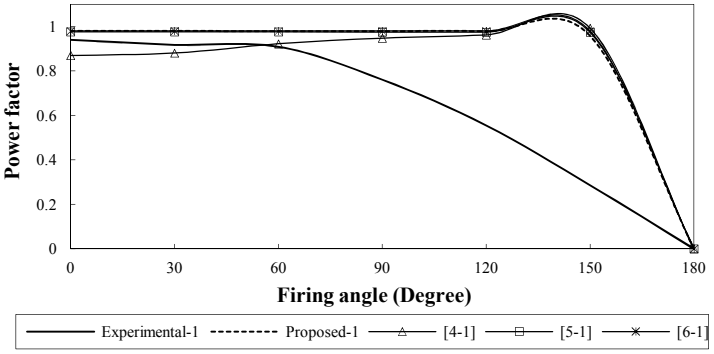

Fig. 14. Power factor of motor-2 using scheme-1 with proposed and conventional methods, at different firing angles.

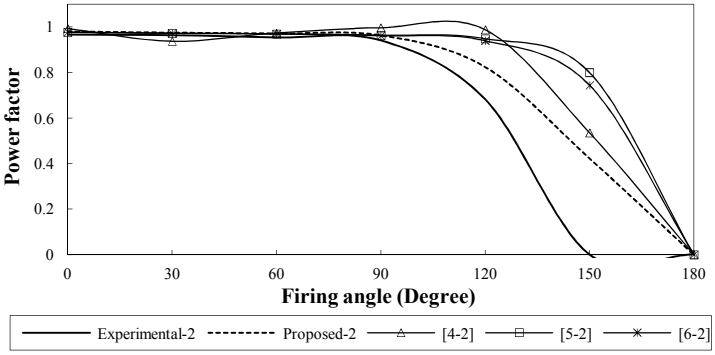

Fig. 15. Power factor of motor-2 using scheme-2 with proposed and conventional methods, at different firing angles.

- In traditional phase angle control scheme, both main and auxiliary winding currents are non-sinusoidal (on account of presence of triac in both the paths) and hence input current harmonics increases, which in turn increase the copper loss due to harmonics. For both the motors, the experimental input current for scheme-1 is more than as for scheme-2, as shown in Figs. 16 and 17, respectively.

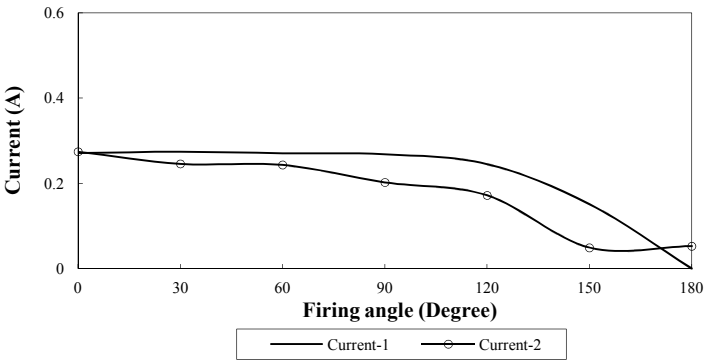

Fig. 16. Comparison of experimental currents of motor-1 using scheme-1 and scheme-2, at different firing angles.

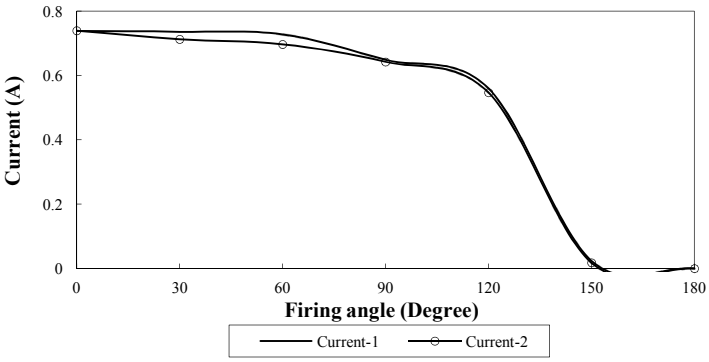

Fig. 17. Comparison of experimental currents of motor-2 using scheme-1 and scheme-2, at different firing angles.

- For advanced phase angle control scheme, the auxiliary winding current is sinusoidal (due to absence of triac in this path) and the main winding current is distorted. Hence, the phasor sum of main and auxiliary winding currents contains fewer harmonic, which further lessens the copper loss due to harmonics. This decreases the consumed input power which can be seen for both the motors in Figs. 18 and 19, respectively.

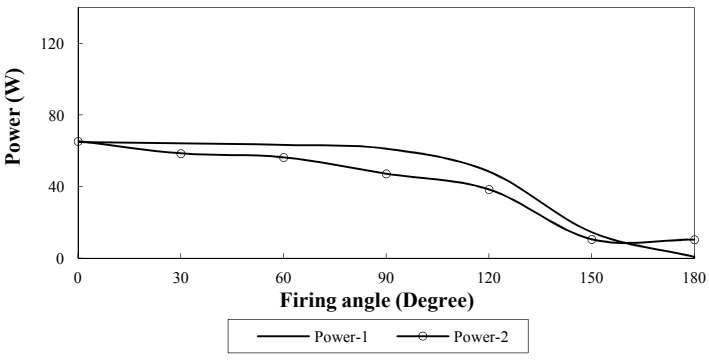

Fig. 18. Comparison of experimental powers of motor-1 using scheme-1 and scheme-2, at different firing angles.

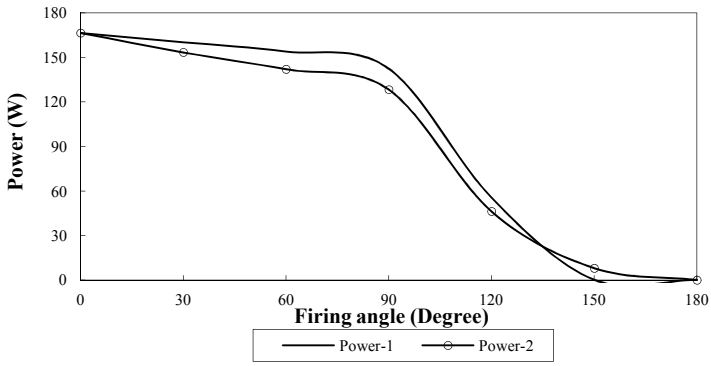

Fig. 19. Comparison of experimental powers of motor-2 using scheme-1 and scheme-2, at different firing angles.

- The absence of harmonics flux in auxiliary winding ameliorates the displacement factor, which improves the power factor for the advanced phase angle control scheme as compared to traditional phase angle control scheme, as shown for both the motors, in Figs. 20 and 21, respectively.

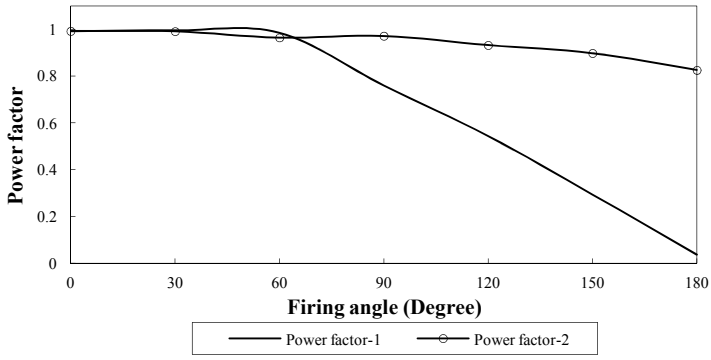

Fig. 20. Comparison of experimental power factors of motor-1 using scheme-1 and scheme-2, at different firing angles.

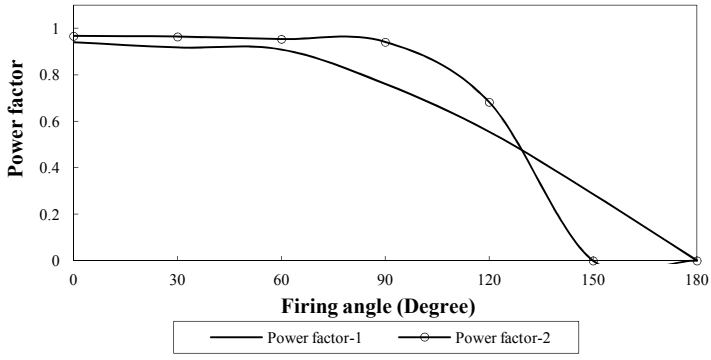

Fig. 21. Comparison of experimental power factors of motor-2 using scheme-1 and scheme-2, at different firing angles.

- Although, the experimental observations distinctly manifest the superior performance of the advanced phase angle control schemes as evidenced from Figs. 16-23, nevertheless, the deficiency appears while the motor parameters are extracted using the conventional methods [4-6], the resulting performance variables (line current, power and power factor) give error vis-a-vis experimentally measured values. However, the

performance variables derived from proposed method give less error to the experimental values.

By exerting the conventional [4-6] and proposed methods to the studied sample motors, for both the energy efficient schemes, the efficiency versus firing angle is obtained as in Figs. 22 and 23. The observations of these Figs. reveal the following points:

- The efficiency of the motor using the conventional methods [4-6], shows no improvement even while using the advanced phase angle control scheme. This indicates the deficiency of the conventional theoretical performance prediction methods.
- The efficiency of the motor shows superiority of scheme-2 over scheme-1, using the proposed method, which is in compliance to earlier work [8] and also confirms the validity of the analytical findings.

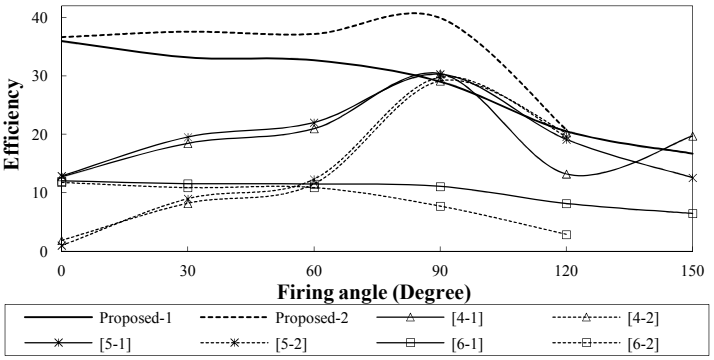

Fig. 22. Calculated performance of motor-1 using scheme-1 and scheme-2 with proposed and conventional results, at different firing angles.

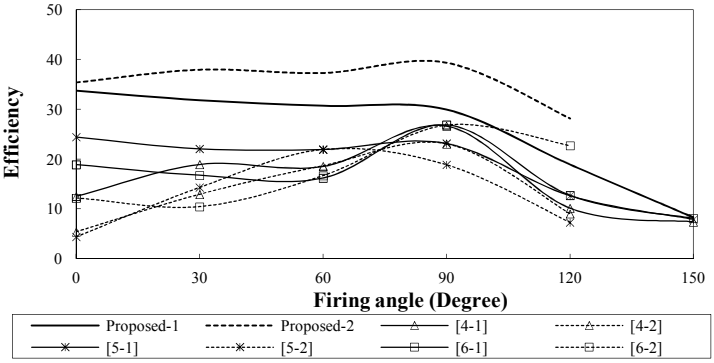

Fig. 23. Calculated performance of motor-2 using scheme-1 and scheme-2 with proposed and conventional results, at different firing angles.

For quantitative result analysis, mean absolute percentage error (MAPE) of performance variables (current, power and power factor) with respect to experimental observations using conventional [4-6] and the proposed method for both the motors and phase angle control schemes are depicted separately, in Table II.

$$MAPE = \sum \left[\frac{100 \times |E_N - T_N|}{E_N} \right] \quad (33)$$

where, E_N, is the experimentally measured performance variable and T_N, is the theoretically obtained performance variable. This table demonstrates that the MAPE of performance variables with respect to experimental observations using the proposed performance prediction method is less than that using the conventional performance prediction methods.

5. CASE STUDY

The equivalent circuit parameters have been determined and hence performance variables are evaluated for four-pole PSCRSPIM with the following ratings and data: 220-240 V, 65 W, 50 Hz, 1400 rpm. Direct dc test, no-load test and locked

rotor tests have provided the following data: R_{sm}= 357.14 Ω, R_{sa}= 357.14Ω, R_s= 178.51Ω, V_{NL}= 240V, I_{NL}= 0.279A, P_{NL}= 65.07W, V_{LR}= 165.43V, I_{LR}= 0.230A, P_{LR}= 37.976W, C= 1.57μF, R_c= 22.4Ω. Winding ratio test has given the following data: E_m= 240V, E_{am}= 198V, E_a=234V, E_{mm}=196V. Experimentally measured performance variables are: V =240V, I_L=0.271A, P_{in}=65W, pf = 0.99. This motor is taken for detailed analysis from section V, depicted in Table I as motor 1. At rated voltage and zero degree triac firing angle, the line currents of the motor for both the schemes, for obvious reason, are sinusoidal. Consequently, the equivalent circuit parameters and performance variables of the motor for both the schemes would remain same. At any firing angle other than zero degree, the line current of motor for scheme-1 and main winding current of the motor for scheme-2 become non-sinusoidal. Hence, for the case study, the equivalent circuit parameters and performance variables of the motor are evaluated for both the schemes at rated voltage on sixty degree firing angle of the triac. The values of line current, power factor, power consumed and efficiency have been evaluated in Table III, using the conventional [4-6] as well as the proposed techniques.

6. CONCLUSION

Conventional parameter estimation method for PSCRSPIM is inadequate to find the performance variables like input current, power factor and power consumed and hence towards the overall performance prediction of the motor at different firing angles of triac (for a triac based ac voltage controller). The proposed method treats the turns ratio as a complex quantity termed as CCVR and the performance variables of the motor have been calculated using this complex quantity. The conventional and proposed methods are used to find the equivalent circuit parameters, input performance variables and hence for the computation of the motor efficiency. Two experimental energy efficient schemes have been used to observe the motor performance at different

firing angles of triac. However, with the conventional performance prediction methods, the input variables show deviation from the experimental results obtained and the estimated efficiency violates the theme of superior performance of the motor with advanced phase angle control scheme. The proposed performance prediction method not only give the performance variables closer to the experimental results but also conform to the superiority of the advanced phase angle control scheme, which validate the analytical findings.

Table 2: Mean Absolute percentage error with respect to experimental

Performance variables	MAPE Motor 1		MAPE Motor 2	
	Scheme 1	Scheme 2	Scheme 1	Scheme 2
Current ([4])	35.939	54.284	17.6640	14.8938
Current ([5])	35.048	53.904	15.5033	14.4932
Current ([6])	89.053	96.630	3.6651	2.9956
Current (Proposed)	20.100	17.280	2.3828	1.3543
Power ([4])	40.028	18.163	13.5933	43.5943
Power ([5])	39.199	18.383	24.6923	30.8076
Power ([6])	82.911	81.789	18.955	28.4107
Power(Proposed)	24.494	12.918	8.1653	21.9798
Power Factor ([4])	65.011	17.894	59.6252	11.6299
Power Factor ([5])	65.014	18.074	60.3700	8.9840
Power Factor ([6])	35.939	21.944	61.1016	8.6973
Power Factor (Proposed)	35.048	4.2669	59.8426	5.5199

Table 3: Case study solutions (At 60 degree firing angle) using conventional and proposed technique

Parameters	Scheme-1 [4]	Scheme-1 [5]	Scheme-1 [6]	Scheme-1 [Proposed]	Scheme-2 [4]	Scheme-2 [5]	Scheme-2 [6]	Scheme-2 [Proposed]
R_s	178.51	178.51	178.51	178.51	178.51	178.51	178.51	178.51
X_s	34.22	34.22	68.44	34.22	34.22	34.22	68.44	34.22
X_r	34.2213	34.22	34.22	34.22	34.22	34.22	34.22	34.22
R_r	371.726	357.07	267.81	535.63	371.72	357.07	371.72	535.63
V_{ab1}	225.6784	225.67	Not Used	225.67	225.67	225.67	Not Used	225.67
X_{mm}	1617.8	1617.8	100.27	1617.8	1617.8	1617.8	100.27	1617.8
$\overline{Z}_{fm}$	328.90 + j633.49	336.16 + j622.26	2.24 + j50	257.85 + j713.45	253.23 + j717.35	261.1 + j710.64	1.52 + j50.07	186.94 + j761.99
$\overline{Z}_{bm}$	93.47 + j27.94	89.88 + j27.090	18.65 + j32.52	132.67 + j39.63	91.63 + j27.50	85.11 + j26.68	1867.67 + j32.14	130.15 + j38.75
$\overline{Z}_{sm}$	357.14+j34.22	357.14+j34.22	357.14 + j68.44	357.14 + j34.22	357.14 + j34.22	357.14 + j34.22	357.14 + j68.44	357.14 + j34.2
$\overline{Z}_{insm}$	779.51 + j695.65	783.19+j683.57	378.05 + j150.96	747.66 + j787.37	702.01 + j779.08	706.36 + j771.54	377.34 + j150.66	674.23 + j834.96
V_{ab2}	Not Used	Not Used	Not Used	803.48	Not Used	Not Used	Not Used	803.48
X_{ma}	Not Used	Not Used	Not Used	5759.7	Not Used	Not Used	Not Used	5759.7
$\overline{Z}_{fa}$	Not Used	Not Used	Not Used	1384.1 + j1083.3	Not Used	Not Used	Not Used	1419.8 + j1630.8
$\overline{Z}_{ba}$	Not Used	Not Used	Not Used	140.44 +	Not Used	Not Used	Not Used	1376.2 +

				j23.91				j23.64
$\overline{Z}_{sa}$	Not Used	Not Used	Not Used	357.14 + j34.22	Not Used	Not Used	Not Used	357.14 + j34.22
$\overline{Z}_{insa}$	Not Used	Not Used	Not Used	1904.1 - j929.56	Not Used	Not Used	Not Used	1936.9 - j382.34
$\overline{I}_1$	Not Used	Not Used	Not Used	0.13 - j0.17	Not Used	Not Used	Not Used	0.13 - j0.17
$\overline{I}_2$	Not Used	Not Used	Not Used	0.05 - j0.06	Not Used	Not Used	Not Used	0.05 - j0.06
$\overline{E}_{ac}$	Not Used	Not Used	Not Used	603.56 - j66.64	Not Used	Not Used	Not Used	603.56 - j66.64
$\overline{E}_{mc}$	Not Used	Not Used	Not Used	90.35 + j9.97	Not Used	Not Used	Not Used	90.35 + j9.97
E_m	240	240	240	Not Used	240	240	240	Not Used
E_{am}	198	198	198	Not Used	198	198	198	Not Used
E_a	234	234	234	Not Used	234	234	234	Not Used
E_{mm}	196	196	196	Not Used	196	196	196	Not Used
a	0.99	0.9924	0.9924	Not Used	0.9924	0.9924	0.9924	Not Used
$\overline{a}$	Not Used	Not Used	Not Used	2.65 - j0.28	Not Used	Not Used	Not Used	2.65 - j0.28
I_L	0.19	0.19	0.55	0.27	0.17	0.17	0.53	0.26
P_{in}	44.67	45.25	127.47	62.02	40.99	41.31	117.04	59.04
pf	1	1	0.98	0.99	0.99	1	0.98	0.98
P_{cu}	4.15	3.78	82.78	12.20	8.38	8.08	87.84	10.31
P_{cl}	23.65	23.65	23.65	23.65	21.85	21.85	21.85	21.85
P_{fwl}	4.46	4.73	6.37	1.44	4.21	4.46	5.95	1.48
P_o	9.37	9.96	14.63	20.25	4.72	5.08	12.76	23.33
η	20.97	22.02	11.48	32.65	11.52	12.30	10.90	37.16

References

[1] *IEEE Standard Test Procedure for Single-Phase Induction Motors*, IEEE Standard 114, 1982.

[2] *IEEE Standard Test Procedure for Single-Phase Induction Motors*, IEEE Standard 114, 2002.

[3] Ghial V. K., Saini L. M., Saini J. S.: *Parameter Estimation of Permanent-Split Capacitor-Run Single-Phase Induction Motor Using Computed Complex Voltage Ratio*. In: IEEE Transaction on Industrial Electronics (2014), vol. 61, no. 2, February 2014, p. 682 – 692.

[4] Matsch L. W.: *Electromagnetic and Electromechanical Machines*, Harper and Row, New York, 1997.

[5] Toro V. D.: *Electric Machines and Power Systems*, Prentice Hall, 1988.

[6] Brosan G. S., Hayden J. T.: *Advanced Electrical Power & Machines*, Sir Isaac Pitman & Sons Ltd., London, 1966.

[7] Toliyat H. A., Levi E., Raina M.: *A review of RFO induction motor parameter estimation techniques*, In: IEEE Transaction on Energy Conversion (2003),, vol. 18, no. 2, June 2003, p. 271 – 283.

[8] Asghari B., Dinavahi V.: *Experimental Validation of a Geometrical Nonlinear Permeance Network Based Real-Time Induction Machine Model*, IEEE Transaction on Industrial Electronics (2012), vol. 59, no. 11, November 2012, p. 4049-4062.

[9] Kowalska T. O., Dybkowski M.: *Stator-current-based MRAS estimator for a wide range speed-sensorless induction-motor drive*, In: IEEE Transaction on Industrial Electronics (2010), vol. 57, no. 4, April 2010, p. 1296 – 1308.

[10] Zaky M. S., Khater M. M., Shokralla S. S., Yasin H. A.: *Wide-speed-range estimation with online parameter identification schemes of sensorless induction motor drives*, In: IEEE Transaction on Industrial Electronics (2009), vol. 56, no. 5, May 2009, pp. 1699 – 1707.

[11] Toliyat H. A., Wlas M., Krzemiriski Z.: *Neural-Network-Based Parameter Estimations of Induction Motors*, In: IEEE Trans. on Industrial Electronics (2008), vol. 55, no. 4, April 2008, p. 1783-1794.

[12] Lee K. B., Blaabjerg F.: *Sensorless DTC-SVM for Induction Motor Driven by a Matrix Converter Using a Parameter Estimation Strategy*, In: IEEE Transaction on Industrial Electronics (2008), vol. 55, no. 2, February 2008, p. 512-521.

[13] Duran M. J., Duran J. L., Perez F., Fernandez J.: *Induction-motor sensorless vector control with online parameter estimation and overcurrent protection*, In: IEEE Transaction on Industrial Electronics (2006), vol. 53, no. 1, February 2006, p. 154-161.

[14] He Y., Wang Y., Feng Y., Wang Z.: *Parameter Identification of an Induction Machine at Standstill Using the Vector Constructing Method*, In: IEEE Transaction on Industrial Electronics (2012), vol. 27, no. 2, February 2012, p. 905-915.

[15] Lin W. M., Su T.J., Wu R. C.: *Parameter Identification of Induction Machine With a Starting No-Load Low-Voltage Test*, In: IEEE Transaction on Industrial Electronics (2012), vol. 59, no. 1 (January 2012), p. 352-360.

[16] Boglietti A., Cavagnino A., Lazzari M.: *Computational Algorithms for Induction-Motor Equivalent Circuit Parameter Determination—Part I: Resistances and Leakage Reactances*, In: IEEE Transaction on Industrial Electronics (2011), vol. 58, no. 9, September 2011, p. 3723-3733.

[17] Boglietti A., Cavagnino A., Lazzari M.: *Computational Algorithms for Induction Motor Equivalent Circuit Parameter Determination—Part II: Skin Effect and Magnetizing Characteristics*, In: IEEE Transaction on Industrial Electronics (2011), vol. 58, no. 9, September 2011, p. 3734-3740.

[18] Gao Z., Colby R. S., Turner L., Leprettre B.: *Filter Design for Estimating Parameters of Induction Motors With Time-Varying Loads*, In: IEEE Transaction on Industrial Electronics (2011), vol. 58, Issue 5, May 2011, p. 1518-1529.

[19] Kwon Y. S., Lee J. H., Moon S. H., Kwon B. K., Choi C. H., Seok, J. K.: *Standstill Parameter Identification of Vector-Controlled Induction Motors Using the Frequency Characteristics of Rotor Bars*, In: IEEE Trans. on Industrial Electronics (2009), vol. 45, no. 5, September/October 2009, p. 1610-1618.

[20] Trentin A., Zanchetta P., Gerada C., Clare J., Wheeler P. W.: *Optimized Commissioning Method for Enhanced Vector Control of High-Power Induction Motor Drives*, In: IEEE Transaction on Industrial Electronics (2009), vol. 56, no. 5, May 2009, p. 1708-1717.

[21] Babau R., Miller T. J. E., Muntean N.: *Complete Parameter Identification of Large Induction Machines From No-Load Acceleration–Deceleration Tests*, In: IEEE Transaction on Industrial Electronics (2007), vol. 54, no. 4, August 2007, p. 1962-1972.

[22] Bachir S., Tnani S., Trigeassou J. C., Champenois G.: *Diagnosis by Parameter Estimation of Stator and Rotor Faults Occurring in Induction Machines*, In: IEEE Trans. on Industrial Electronics (2006), vol. 53, no. 3, June 2006, p. 963-973.

[23] Vaclavek P., Blaha P.: *Lyapunov-function-based flux and speed observer for AC induction motor sensorless control and parameters estimation*, In: IEEE Transaction on Industrial Electronics (2006), vol. 53, no. 1, February 2006, p. 138-145.

[24] Saejia M., Sangwongwanich S.: *Averaging Analysis Approach for Stability Analysis of Speed-Sensorless Induction Motor Drives With Stator Resistance Estimation*, In: IEEE Transaction on Industrial Electronics (2006), vol. 53, no. 1, February 2006, p. 162- 177.

[25] Jacobina C. B., Filho J. E. C., Lima A. M. N.: *Estimating the Parameters of Induction Machines at Standstill*, In: IEEE Transaction on Energy Conversion (2002), vol. 17, no. 1, March 2002, pp. 85-89.

[26] Umans S. D.: *Steady-state, lumped-parameter model for capacitor-run, single-phase induction motors*, In: IEEE Trans. on Industry Applications (1996), vol. 32, no. 1, January/February 1996, p. 169-179.

[27] Merwe C. V. D., Merwe F. S. V. D.: *A study of methods to measure parameters of single phase induction motors*, In: IEEE Trans. Energy Conversion (1995), vol. 10, no. 2, June 1995, p. 248-253.

[28] Ilango G. S., Samidurai K., Roykumar M., Thanushkodi K.: *Energy efficient power electronic controller for a capacitor-run single-phase induction motor*, In: Energy Conversion and Management (2009), vol. 50, Issue. 9, September 2009, p. 2152-2157.

[29] Sundareswaran, K.: *Performance Comparison of Capacitor-Run Induction Motors Supplied From AC Voltage Regulator and SPWM AC Chopper*, In: IEEE Trans. on Industrial Electronics (2006), vol. 53, no. 3, June 2006, p. 990-993.

[30] Sundareswaran, K.: *An improved energy-saving scheme for capacitor-run induction motor*, In: IEEE Trans. on Industrial Electronics (2001), vol. 48, no. 1, February 2001, p. 238-240.